

Physics of Transcendental Numbers as Forming Factor of the Solar System

Hartmut Müller

Rome, Italy.

E-mail: hm@interscalar.com

Transcendental ratios of physical quantities can inhibit the occurrence of destabilizing parametric resonance and in this way, provide stability in systems of coupled periodic processes. In this paper we apply this approach to the solar system and show that it can explain the current set of rotational and orbital periods and distances including observed tendencies of their evolution.

Introduction

One of the unsolved fundamental problems in physics [1] is the stability of systems of a large number of coupled periodic processes, for instance, the stability of planetary systems. If numerous bodies are gravitationally bound to one another, perturbation models predict long-term highly unstable states [2] that contradict the physical reality of the solar system and thousands of exoplanetary systems.

Another issue is that in theory, there are infinitely many pairs of orbital periods and distances that fulfill Kepler's laws. Regrettably, Einstein's field equations do not reduce the theoretical variety of possible orbits, but increases it even more. As a consequence, the current orbital system of the Sun seems to be accidental, and its stability a miracle.

Furthermore, there is no known law concerning the rotation of celestial bodies besides conservation of the angular momentum [3] that they retain from the protoplanetary disk, so that also the current distribution of the rotational periods appears as to be accidental.

However, many planets in extrasolar systems like Trappist 1 or Kepler 20 have almost the same orbital periods as the large moons of Jupiter, Saturn, Uranus and Neptune [4]. Trappist 1 is 40 light years away from our solar system [5] and Kepler 20 nearly 1000 light years [6].

The question is, why they prefer similar orbital periods if there are infinite possibilities? Obviously, there are orbital periods preferred anywhere in the galaxy. Why these orbital periods are preferred? What makes them attractive?

In this paper, we introduce an approach to the problem of stability based on the physical interpretation of certain statements of number theory. This approach leads us to the conclusion that in real systems, bound periodic processes approximate transcendental frequency ratios that allow them to avoid destabilizing parametric resonance. We illustrate this conclusion on some well-known features of the solar system which are still unexplained.

Theoretical Approach

The starting point of our approach is the measurement as it is the source of data that allow us developing and proofing theoretical models of the reality. The result of a measure-

ment is the ratio of physical quantities where one of them is the reference quantity called unit of measurement. Whether measuring a wavelength or phase, a frequency, the speed or duration of some process, the mass of a body or its temperature, initially this ratio is a real number, regardless of its subsequent interpretation as component of a vector or tensor, for example. As real value, this ratio can approximate an integer, rational, irrational algebraic or transcendental number. In [7] we have shown that the difference between rational, irrational algebraic and transcendental numbers is not only a mathematical task, but it is also an essential aspect of stability in systems of bound periodic processes. For instance, integer frequency ratios, in particular fractions of small integers, make possible parametric resonance that can destabilize such a system [8, 9]. For instance, asteroids cannot maintain orbits that are unstable because of their resonance with Jupiter [10]. These orbits form the Kirkwood Gaps, which are areas in the asteroid belt where asteroids are absent.

According to this idea, irrational ratios should not cause destabilizing resonance interactions, because irrational numbers cannot be represented as a ratio of integers. However, algebraic irrational numbers, being real roots of algebraic equations, can be converted to rational numbers by multiplication. For example, the algebraic irrational number $\sqrt{2} = 1.41421 \dots$ cannot become a frequency scaling factor in real systems of coupled periodic processes, because $\sqrt{2} \cdot \sqrt{2} = 2$ creates the conditions for the occurrence of parametric resonance. Thus, only transcendental ratios can prevent parametric resonance, because they cannot be converted to rational or integer numbers by multiplication.

Actually, it is transcendental numbers, that define the preferred frequency ratios which allow to avoid destabilizing resonance [11]. In this way, transcendental frequency ratios sustain the lasting stability of coupled periodic processes. With reference to the evolution of a planetary system and its stability, we may therefore expect that the ratio of any two orbital periods should finally approximate a transcendental number.

Among all transcendental numbers, Euler's number $e = 2.71828 \dots$ is unique, because its real power function e^x coincides with its own derivatives. In the consequence, Euler's number allows inhibiting parametric resonance between any coupled periodic processes including their derivatives.

Because of this unique property of Euler’s number, we expect that periodic processes in real systems prefer frequency ratios close to Euler’s number and its roots. The natural logarithms of those frequency ratios are therefore close to integer $0, \pm 1, \pm 2, \dots$ or rational $\pm 1/2, \pm 1/3, \pm 1/4, \dots$ values. For rational exponents, the natural exponential function is always transcendental [12]. As shown by A. Khinchine [13], any rational number has a biunique presentation as a finite continued fraction. Consequently, we can present the natural logarithms of the frequency ratios we are looking for as finite continued fractions:

$$\ln(\omega_A/\omega_B) = \mathcal{F} = \langle n_0; n_1, n_2, \dots, n_k \rangle \quad (1)$$

ω_A and ω_B are the angular frequencies of two bound periodic processes A and B avoiding parametric resonance. We use angle brackets for continued fractions. All denominators n_1, n_2, \dots, n_k of a continued fraction including the free link n_0 are integer numbers. All numerators equal 1. The length of a continued fraction is given by the number k of layers.

Finite continued fractions represent all rational numbers in the sense that there is no rational number that cannot be represented by a finite continued fraction. This universality of continued fractions evidences that the distribution of rational logarithms (1) in the number continuum is fractal.

The first layer of this fractal is given by the truncated after n_1 continued fractions:

$$\langle n_0; n_1 \rangle = n_0 + \frac{1}{n_1}$$

The denominators n_1 follow the sequence of integer numbers $\pm 1, \pm 2, \pm 3$ etc. The second layer is given by the truncated after n_2 continued fractions:

$$\langle n_0; n_1, n_2 \rangle = n_0 + \frac{1}{n_1 + \frac{1}{n_2}}$$

Figure 1 shows the first and the second layer in comparison. As we can see, reciprocal integers $\pm 1/2, \pm 1/3, \pm 1/4, \dots$ are the attractor points of the fractal. In these points, the distribution density of rational logarithms (1) reaches a local maximum. Integers $0, \pm 1, \pm 2, \dots$ define the main attractors. Consequently, integer arguments of the natural exponential function define attractor points of transcendental numbers and ranges of stability that allow bound periodic processes to avoid parametric resonance.

Figure 1 shows that integer logarithms $0, \pm 1, \pm 2, \dots$ form the widest ranges of stability. Half logarithms $\pm 1/2$ form smaller ranges, third logarithms $\pm 1/3$ form the next smaller ranges and fourth logarithms $\pm 1/4$ form even smaller ranges of stability etc. Increasing the length of the continued fraction (1), the distribution density of the transcendental frequency

ratios ω_A/ω_B is increasing as well. Nevertheless, their distribution is not homogeneous, but fractal. Applying continued fractions and truncating them, we can represent the logarithms $\ln(\omega_A/\omega_B)$ as rational numbers $\langle n_0; n_1, n_2, \dots, n_k \rangle$ and make visible their fractal distribution.

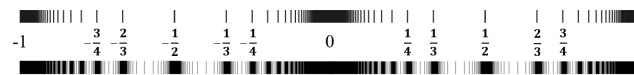


Fig. 1: The distribution of rational logarithms for $k = 1$ (above) and for $k = 2$ (below) in the range $-1 \leq \mathcal{F} \leq 1$.

Here I would like to underline that the application of continued fractions doesn’t limit the universality of our conclusions, because continued fractions deliver biunique representations of all real numbers including transcendental. Therefore, the fractal distribution of transcendental ratios (1) is an inherent feature of the number continuum that we call the *Fundamental Fractal* [11].

The natural exponential function $\exp(\mathcal{F})$ of the rational argument $\mathcal{F} = \langle n_0; n_1, n_2, \dots, n_k \rangle$ generates a fractal set of transcendental frequency ratios $\omega_A/\omega_B = \exp(\mathcal{F})$ which allow to avoid destabilizing parametric resonance and in this way, provide the lasting stability of periodic processes bound in systems regardless of their complexity. This conclusion we have exemplified [14] in particle physics, astrophysics, geophysics, biophysics and engineering.

For bound harmonic quantum oscillators, the continued fractions \mathcal{F} define not only ratios of frequencies ω , oscillation periods $\tau = 1/\omega$ and wavelengths $\lambda = c/\omega$, but also ratios of accelerations $a = c \cdot \omega$, energies $E = \hbar \cdot \omega$ and masses $m = \omega \cdot \hbar/c^2$, which allow to avoid parametric resonance.

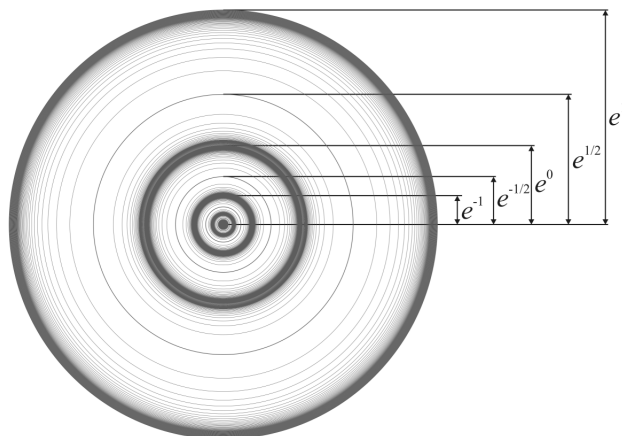


Fig. 2: The first layer ($k = 1$) of equipotential surfaces of the Fundamental Field in the 2D-projection in the range $-1 \leq \mathcal{F} \leq 1$.

The spatio-temporal projection of the Fundamental Fractal \mathcal{F} is a fractal scalar field of transcendental attractors, the *Fundamental Field* [15]. The connection between the spatial and temporal projections is given by the speed of light $c = 299792458$ m/s. The constancy of c makes both projections isomorphic, so that there is no arithmetic or geometric

difference. Only the units of measurement are different. Figure 2 shows the 2D-projection $\exp(\mathcal{F})$ of its first layer. The Fundamental Field is topologically 3-dimensional, a fractal set of embedded spheric equipotential surfaces. The logarithmic potential difference defines a gradient directed to the center of the field that causes a central force of attraction creating the effect of a field source. Because of the fractal logarithmic hyperbolic metric of the field, also every equipotential surface is an attractor. The logarithmic scalar potential difference $\Delta\mathcal{F}$ of sequent equipotential surfaces equals the difference of sequent continued fractions (1) on a given layer:

$$\Delta\mathcal{F} = \langle n_0; n_1, \dots, n_k \rangle - \langle n_0; n_1, \dots, n_k + 1 \rangle$$

Main equipotential surfaces at $k = 0$ correspond with integer logarithms (1); equipotential surfaces at deeper layers $k > 0$ correspond with rational logarithms.

The Fundamental Field is of pure arithmetic origin, and there is no particular physical mechanism required as field source. It is all about transcendental ratios of frequencies [11] that allow coupled periodic processes to avoid destabilizing parametric resonance. Hence, the Fundamental Field concerns all repetitive processes which share at least one characteristic – the frequency. Therefore, we postulate the universality of the Fundamental Field that affects any type of physical interaction, regardless of its complexity.

PROPERTY	ELECTRON	PROTON
$E = mc^2$	0.5109989461(31) MeV	938.2720813(58) MeV
$\omega = E/\hbar$	$7.76344 \cdot 10^{20}$ Hz	$1.42549 \cdot 10^{24}$ Hz
$\tau = 1/\omega$	$1.28809 \cdot 10^{-21}$ s	$7.01515 \cdot 10^{-25}$ s
$\lambda = c/\omega$	$3.86159 \cdot 10^{-13}$ m	$2.10309 \cdot 10^{-16}$ m

Table 1: The basic set of physical properties of the electron and proton. Data from Particle Data Group [21]. Frequencies, oscillation periods and wavelengths are calculated.

In fact, scale relations in particle physics [16, 17], nuclear physics [18, 19] and astrophysics [15, 20] obey the same Fundamental Fractal (1), without any additional or particular settings. The proton-to-electron rest energy ratio approximates the first layer of the Fundamental Fractal that could explain their exceptional stability [14]. Normal matter is formed by nucleons and electrons because they are exceptionally stable quantum oscillators. In the concept of isospin, proton and neutron are viewed as two states of the same quantum oscillator. Furthermore, they have similar rest masses. However, a free neutron decays into a proton and an electron within 15 minutes while the life-spans of the proton and electron top everything that is measurable, exceeding 10^{29} years [21]. The proton-to-electron ratio (tab. 1) approximates the seventh

power of Euler’s number and its square root:

$$\ln\left(\frac{E_p}{E_e}\right) = \ln\left(\frac{938.2720813 \text{ MeV}}{0.5109989 \text{ MeV}}\right) \approx 7 + \frac{1}{2} = \langle 7; 2 \rangle$$

In the consequence of this potential difference of the proton relative to the electron, the scaling factor \sqrt{e} connects attractors of proton stability with similar attractors of electron stability in alternating sequence.

Applying Khinchine’s [13] continued fraction method, we get the best approximation of the proton-to-electron ratio:

$$\ln\left(\frac{E_p}{E_e}\right) = 7 + \frac{1}{2} + \frac{1}{64 + \frac{1}{11}} = 7.515427769 \dots$$

Recent data [22] of the proton-to-electron ratio define the upper limit as 7.515427773 and the lower limit 7.515427702. The same method delivers for the neutron-to-proton ratio:

$$\ln\left(\frac{E_n}{E_p}\right) = \frac{1}{726}$$

By the way, $726 = 11 \cdot 11 \cdot 6$. The denominator 11 appears also in the W/Z-to-electron ratio [11], for example:

$$\ln\left(\frac{E_Z}{E_e}\right) = 12 + \frac{1}{11}$$

The unique properties of the electron and proton predestinate their physical characteristics as fundamental units. Table 1 shows the basic set of electron and proton units that can be considered as a *Fundamental Metrology* (c is the speed of light in a vacuum, \hbar is the Planck constant). In [23] was shown that the fundamental metrology (tab. 1) is completely compatible with Planck units [24]. Originally proposed in 1899 by Max Planck, these units are also known as natural units, because the origin of their definition comes only from properties of nature and not from any human construct. Max Planck wrote [25] that these units, “regardless of any particular bodies or substances, retain their importance for all times and for all cultures, including alien and non-human, and can therefore be called natural units of measurement”. Planck units reflect the characteristics of space-time.

We hypothesize that scale invariance according the Fundamental Fractal (1) calibrated on the physical properties of the proton and electron is a universal characteristic of organized matter and criterion of stability. This hypothesis we have called *Global Scaling* [14].

On this background, atoms and molecules emerge as stable eigenstates in fractal chain systems of harmonically oscillating protons and electrons. Andreas Ries [18] demonstrated that this model allows for the prediction of the most abundant isotope of a given chemical element.

In the following, we use the symbol \mathcal{F}_e for the Fundamental Fractal (1) calibrated on the properties of the electron,

and the symbol \mathcal{F}_p for the Fundamental Fractal calibrated on the properties of the proton. For example, $\mathcal{F}_e\langle 66 \rangle$ means the main attractor 66 of electron stability. In the solar system, this attractor stabilizes the orbital period of Jupiter [7].

In [15] we applied the Fundamental Fractal (1) to planetary systems interpreting gravity as macroscopic attractor effect of transcendental frequency ratios in chain systems of harmonic quantum oscillators – protons and electrons. In [26] we demonstrated that the Fundamental Field (fig. 2) in the interval of the main attractors $\langle 49 \rangle \leq \mathcal{F}_p \leq \langle 52 \rangle$ of proton stability reproduces the 3D profile of the Earth's interior confirmed by seismic exploration. As well, the stratification layers in planetary atmospheres follow the Fundamental Field [27]. In [28] we have shown that the Fundamental Fractal determines the Earth axial precession cycle, the obliquity variation cycle as well as the apsidal precession cycle and the orbital eccentricity cycle. There we have also shown that recently discovered geological cycles, like the 27 million years' cycle [29], as well as the periodic variations in the movement of the Solar system through the Galaxy, substantiate their determination by the Fundamental Fractal.

The orbital and rotational periods of planets, planetoids and large moons of the solar system correspond with attractors of electron and proton stability [23]. This is valid also for exoplanets [4] of the systems Trappist 1 and Kepler 20. In [15] we have shown that the maxima in the frequency distribution of the orbital periods of 1430 exoplanets listed in [30] correspond with attractors of the Fundamental Fractal. As well, the maxima in the frequency distribution of the number of stars in the solar neighborhood as function of the distance between them correspond with attractors of the Fundamental Fractal [20].

Exemplary applications

Jupiter's orbital period $T_O(\text{Jupiter}) = 4332.59$ days [31] approximates the main attractor $\mathcal{F}_e\langle 66 \rangle$ of electron stability that equals the 66th power of Euler's number multiplied by the oscillation period of the electron (see tab. 1):

$$\ln\left(\frac{T_O(\text{Jupiter})}{2\pi \cdot \tau_e}\right) = \ln\left(\frac{4332.59 \cdot 86400 \text{ s}}{2\pi \cdot 1.28809 \cdot 10^{-21} \text{ s}}\right) = 66.00$$

Jupiter's distance from Sun approximates the main equipotential surface $\mathcal{F}_e\langle 56 \rangle$ of electron stability that equals the 56th power of Euler's number multiplied by the Compton wavelength of the electron. The aphelion $5.45492 \text{ AU} = 8.160444 \cdot 10^{11} \text{ m}$ delivers the upper approximation:

$$\ln\left(\frac{A_O(\text{Jupiter})}{\lambda_e}\right) = \ln\left(\frac{8.160444 \cdot 10^{11} \text{ m}}{3.86159 \cdot 10^{-13} \text{ m}}\right) = 56.01$$

The perihelion $4.95029 \text{ AU} = 7.405528 \cdot 10^{11} \text{ m}$ delivers the lower approximation:

$$\ln\left(\frac{P_O(\text{Jupiter})}{\lambda_e}\right) = \ln\left(\frac{7.405528 \cdot 10^{11} \text{ m}}{3.86159 \cdot 10^{-13} \text{ m}}\right) = 55.91$$

Now we can apply Kepler's 3rd law of planetary motion and express the gravitational parameter μ_{Sun} of the Sun through Euler's number, the speed of light c in a vacuum and the oscillation period τ_e of the electron:

$$\mu_{Sun} = \tau_e \cdot c^3 \cdot e^{36}$$

In logarithms, the cube of the mean orbit radius divided by the square of the orbital period $56 \cdot 3 - 66 \cdot 2 = 36$ results in the 36th power of Euler's number. In this way, within our numeric physical approach, the gravitational parameter of the Sun does not appear to be accidental, but is stabilized by Euler's number and origins from the quantum physical properties of the electron.

In a similar way, we can derive the attractor that the gravitational parameter of Jupiter is approximating. Thanks to the negligible eccentricities of the orbits of Jupiter's large moons, we can use the mean orbit radius for calculations. Callisto's orbit radius $R_O(\text{Callisto}) = 1.8827 \cdot 10^9 \text{ m}$ approaches the equipotential surface $\mathcal{F}_e\langle 50 \rangle$ of electron stability:

$$\ln\left(\frac{R_O(\text{Callisto})}{\lambda_e}\right) = \ln\left(\frac{1.8827 \cdot 10^9 \text{ m}}{3.86159 \cdot 10^{-13} \text{ m}}\right) = 49.95$$

Callisto's orbital period $T_O(\text{Callisto}) = 16.689$ days is approaching the attractor $\mathcal{F}_e\langle 60; 2 \rangle$ of electron stability:

$$\ln\left(\frac{T_O(\text{Callisto})}{2\pi \cdot \tau_e}\right) = \ln\left(\frac{16.689 \cdot 86400 \text{ s}}{2\pi \cdot 1.28809 \cdot 10^{-21} \text{ s}}\right) = 60.45$$

For reaching both attractors, Callisto must still increase its orbital period by 10 hours and of course, its mean orbit radius as well. Now we can apply Kepler's 3rd law of planetary motion and express the gravitational parameter $\mu_{Jupiter}$ of Jupiter through Euler's number:

$$\mu_{Jupiter} = \tau_e \cdot c^3 \cdot e^{29}$$

In logarithms, the cube of the mean orbit radius divided by the square of the orbital period $50 \cdot 3 - (60 + 1/2) \cdot 2 = 29$ results in the 29th power of Euler's number. In this way, Jupiter's gravitational parameter approximates the attractor $\mathcal{F}_e\langle 29 \rangle$ of electron stability.

Now we can derive the attractor that the gravitational parameter of the Earth is approximating. The orbital distance of the Moon from Earth approximates the equipotential surface $\mathcal{F}_e\langle 48; 3 \rangle$ of electron stability that equals the 48th power of Euler's number and its cubic root multiplied by the electron wavelength. The apoapsis of the Moon $A_O = 4.067 \cdot 10^8 \text{ m}$ delivers the upper approximation:

$$\ln\left(\frac{A_O(\text{Moon})}{\lambda_e}\right) = \ln\left(\frac{4.067 \cdot 10^8 \text{ m}}{3.86159 \cdot 10^{-13} \text{ m}}\right) = 48.41$$

Periapsis $3.626 \cdot 10^8 \text{ m}$ delivers the lower approximation:

$$\ln\left(\frac{P_O(\text{Moon})}{\lambda_e}\right) = \ln\left(\frac{3.626 \cdot 10^8 \text{ m}}{3.86159 \cdot 10^{-13} \text{ m}}\right) = 48.29$$

The orbital period $T_O(Moon) = 27.32166$ days approaches the main attractor $\mathcal{F}_e\langle 61 \rangle$ of electron stability:

$$\ln\left(\frac{T_O(Moon)}{2\pi \cdot \tau_e}\right) = \ln\left(\frac{27.32166 \cdot 86400 \text{ s}}{2\pi \cdot 1.28809 \cdot 10^{-21} \text{ s}}\right) = 60.95$$

For reaching this attractor, the Moon must increase its distance from Earth, and that's exactly what the Moon does [32]. However, our approach predicts an increase only until Moon's orbital period reaches the main attractor $\mathcal{F}_e\langle 61 \rangle = 29.08$ days. Now we can apply Kepler's 3rd law of planetary motion and express the gravitational parameter μ_{Earth} of the Earth through Euler's number:

$$\mu_{Earth} = \tau_e \cdot c^3 \cdot e^{23}$$

In logarithms, the cube of the mean orbit radius divided by the square of the orbital period $(48 + 1/3) \cdot 3 - 61 \cdot 2 = 23$ results in the 23th power of Euler's number. Consequently, also the gravitational parameter of the Earth does not appear to be accidental, but origins from the quantum physical properties of the electron and is approaching a main attractor of the Fundamental Fractal.

In a similar way, we can derive the attractors that the gravitational parameters of other planets are approximating. Phobos' mean orbit radius approximates the equipotential surface $\mathcal{F}_e\langle 45; -3 \rangle$ while its orbital period is stabilized by the attractor $\mathcal{F}_e\langle 56; 2 \rangle$. Consequently, the gravitational parameter of Mars approximates the attractor $\mathcal{F}_e\langle 21 \rangle$, because $(45 - 1/3) \cdot 3 - (56 + 1/2) \cdot 2 = 21$:

$$\mu_{Mars} = \tau_e \cdot c^3 \cdot e^{21}$$

The gravitational parameter of Uranus approximates the center of scale symmetry $(23 + 29)/2 = 26$ between the gravitational parameters of the Earth $\mathcal{F}_e\langle 23 \rangle$ and Jupiter $\mathcal{F}_e\langle 29 \rangle$:

$$\mu_{Uranus} = \tau_e \cdot c^3 \cdot e^{26}$$

Neptune's gravitational parameter approaches the same attractor $\mathcal{F}_e\langle 26 \rangle$, but for reaching it, Neptune's moon system must become larger. Saturn's gravitational parameter approximates the center of scale symmetry $(26 + 29)/2 = 27 + 1/2$ between the parameters of Uranus $\mathcal{F}_e\langle 26 \rangle$ and Jupiter $\mathcal{F}_e\langle 29 \rangle$:

$$\mu_{Saturn} = \tau_e \cdot c^3 \cdot e^{27+1/2}$$

Because the scaling factor \sqrt{e} links attractors of electron stability to corresponding attractors of proton stability, the mean orbit radius of Saturn's largest moon Titan approximates also the main equipotential surface $\mathcal{F}_p\langle 57 \rangle$. Titan's apoapsis $A_O = 1.25706 \cdot 10^9$ m delivers the upper approximation:

$$\ln\left(\frac{A_O(Titan)}{\lambda_p}\right) = \ln\left(\frac{1.25706 \cdot 10^9 \text{ m}}{2.10309 \cdot 10^{-16} \text{ m}}\right) = 57.05$$

Periapsis $1.18668 \cdot 10^9$ m delivers the lower approximation:

$$\ln\left(\frac{P_O(Titan)}{\lambda_p}\right) = \ln\left(\frac{1.18668 \cdot 10^9 \text{ m}}{2.10309 \cdot 10^{-16} \text{ m}}\right) = 56.99$$

And Titan's orbital period $T_O = 15.945$ days is approaching the main attractor $\mathcal{F}_p\langle 68 \rangle$ of proton stability:

$$\ln\left(\frac{T_O(Titan)}{2\pi \cdot \tau_p}\right) = \ln\left(\frac{15.945 \cdot 86400 \text{ s}}{2\pi \cdot 7.01515 \cdot 10^{-25} \text{ s}}\right) = 67.92$$

In this way, Saturn's gravitational parameter approximates also the attractor $\mathcal{F}_p\langle 35 \rangle$, because $57 \cdot 3 - 68 \cdot 2 = 35$ results in the 35th power of Euler's number, multiplied by the oscillation period of the proton:

$$\mu_{Saturn} = \tau_p \cdot c^3 \cdot e^{35}$$

Besides conservation of angular momentum [33], there is no known law concerning the rotation of celestial bodies. The more remarkable is the correspondence of the rotation periods of planets, planetoids and large moons with attractors of the Fundamental Fractal (1) as shown in [15]. Here we give some of the most expressive examples.

In the solar system, the 66th power of Euler's number stabilizes not only the orbital period 4332.59 days of Jupiter, but also the orbital period 686.971 days of Mars and the rotational period 9.074 hours of the planetoid Ceres, the largest body of the main asteroid belt that orbits the Sun between Mars and Jupiter. The difference lays in the reference units. While in the case of Jupiter's orbital period, the reference unit is the oscillation period of the electron $2\pi\tau_e$, in the case of Mars, it is the angular oscillation period of the electron τ_e :

$$\ln\left(\frac{T_O(Mars)}{\tau_e}\right) = \ln\left(\frac{686.971 \cdot 86400 \text{ s}}{1.28809 \cdot 10^{-21} \text{ s}}\right) = 66.00$$

And in the case of the rotational period of Ceres, the reference unit is the angular oscillation period of the proton τ_p :

$$\ln\left(\frac{T_R(Ceres)}{\tau_p}\right) = \ln\left(\frac{9.07417 \cdot 3600 \text{ s}}{7.01515 \cdot 10^{-25} \text{ s}}\right) = 66.01$$

The rotational periods of Mars and Earth approximate the next main attractor $\mathcal{F}_p\langle 67 \rangle$ of proton stability:

$$\ln\left(\frac{T_R(Mars)}{\tau_p}\right) = \ln\left(\frac{24.62278 \cdot 3600 \text{ s}}{7.01515 \cdot 10^{-25} \text{ s}}\right) = 67.01$$

$$\ln\left(\frac{T_R(Earth)}{\tau_p}\right) = \ln\left(\frac{23.93447 \cdot 3600 \text{ s}}{7.01515 \cdot 10^{-25} \text{ s}}\right) = 66.98$$

Mercury's period 58.64615 days of rotation is approaching the main attractor $\mathcal{F}_p\langle 71 \rangle$. Although Venus rotation is retrograde, its period 243.025 days approximates the attractor $\mathcal{F}_p\langle 72; 2 \rangle$ that coincides with $\mathcal{F}_e\langle 65 \rangle$. The rotation of further planets, planetoids and moons of the solar system we have analyzed in [15].

Conclusion

The application of our numeric-physical approach to the analysis of the orbital and rotational periods of the planets, planetoids and moons of the solar system and thousands of exoplanets [15] leads us to the conclusion that the avoidance of orbital, rotational, proton and electron parametric resonances by approximation of transcendental ratios can be viewed as a basic forming factor of planetary systems.

Studies of circumstellar disks around young stars conclude [34] that the planet formation process is observationally required to be both fast and common. Solid planets in the solar system should have then formed within less than a few million years, which is a major challenge for terrestrial planet formation theories [35].

Perhaps, our approach can explain the fast consolidation of the solar system. In fact, the scale-invariant fractal distribution of transcendental Euler attractors of stability is an inherent feature of the number continuum and therefore given a priori and does not require a long history of random collisions to find them.

The circumstance that the gravitational parameters of the Sun and the planets approximate main numeric attractors of electron and proton stability could be an approach to achieve a deeper understanding of gravitation.

In modern theoretical physics, numerical ratios usually remain outside the realm of theoretical interest. In this work we have tried to elucidate the physical meaning of numerical ratios and to show their theoretical and practical importance.

Acknowledgements

The author is grateful to Leili Khosravi, Simona Muratori, Viktor Panchelyuga, Oleg Kalinin, Viktor Bart and Michael Kauderer for valuable discussions.

Submitted on April 27, 2022

References

- Hansson J. The 10 Biggest Unsolved Problems in Physics. *International Journal of Modern Physics and Applications*, 2015, v. 1, no. 1, 12–16.
- Heggie D. C. The Classical Gravitational N-Body Problem. arXiv: astro-ph/0503600v2, 11 Aug 2005.
- Colombo G. Rotational Period of the Planet Mercury. *Letters to Nature*, 1965, no. 5010, 575.
- Müller H. Global Scaling of Planetary Systems. *Progress in Physics*, 2018, v. 14, 99–105.
- Gillon M. et al. Seven temperate terrestrial planets around the nearby ultracool dwarf star TRAPPIST-1. *Nature*, 2017, v. 542, 456–460.
- Hand E. Kepler discovers first Earth-sized exoplanets. *Nature*, 2011, <https://doi.org/10.1038/nature.2011.9688>
- Müller H. On the Cosmological Significance of Euler's Number. *Progress in Physics*, 2019, v. 15, 17–21.
- Dombrowski K. Rational Numbers Distribution and Resonance. *Progress in Physics*, 2005, v. 1, no. 1, 65–67.
- Panchelyuga V.A., Panchelyuga M. S. Resonance and Fractals on the Real Numbers Set. *Progress in Physics*, 2012, v. 8, no. 4, 48–53.
- Minton D. A., Malhotra R. A record of planet migration in the main asteroid belt. *Nature*, 2009, v. 457, 1109–1111.
- Müller H. The Physics of Transcendental Numbers. *Progress in Physics*, 2019, vol. 15, 148–155.
- Hilbert D. Über die Transcendenz der Zahlen e und π . *Mathematische Annalen*, 1893, v. 43, 216–219.
- Khinchine A. Continued fractions. University of Chicago Press, Chicago, (1964).
- Müller H. Global Scaling. The Fundamentals of Interscalar Cosmology. *New Heritage Publishers*, Brooklyn, New York, USA, ISBN 978-0-9981894-0-6, (2018).
- Müller H. Physics of Transcendental Numbers meets Gravitation. *Progress in Physics*, 2021, v. 17, 83–92.
- Müller H. Fractal Scaling Models of Natural Oscillations in Chain Systems and the Mass Distribution of Particles. *Progress in Physics*, 2010, v. 6, 61–66.
- Müller H. Emergence of Particle Masses in Fractal Scaling Models of Matter. *Progress in Physics*, 2012, v. 8, 44–47.
- Ries A. Qualitative Prediction of Isotope Abundances with the Bipolar Model of Oscillations in a Chain System. *Progress in Physics*, 2015, v. 11, 183–186.
- Ries A., Fook M. Fractal Structure of Nature's Preferred Masses: Application of the Model of Oscillations in a Chain System. *Progress in Physics*, 2010, v. 4, 82–89.
- Müller H. Physics of Transcendental Numbers Determines Star Distribution. *Progress in Physics*, 2021, v. 17, 164–167.
- Zylaet P.A. al. (Particle Data Group), *Prog. Theor. Exp. Phys.*, 083C01, 2020 and 2021 update.
- Physical constants. Particle Data Group, pdg.lbl.gov
- Müller H. Scale-Invariant Models of Natural Oscillations in Chain Systems and their Cosmological Significance. *Progress in Physics*, 2017, v. 13, 187–197.
- Astrophysical constants. Particle Data Group, pdg.lbl.gov
- Planck M. Über Irreversible Strahlungsvorgänge. *Sitzungsbericht der Königlich Preußischen Akademie der Wissenschaften*, 1899, v. 1, 479–480.
- Müller H. Quantum Gravity Aspects of Global Scaling and the Seismic Profile of the Earth. *Progress in Physics*, 2018, v. 14, 41–45.
- Müller H. Global Scaling of Planetary Atmospheres. *Progress in Physics*, 2018, v. 14, 66–70.
- Müller H. Physics of Transcendental Numbers on the Origin of Astrogeophysical Cycles. *Progress in Physics*, 2021, v. 17, 225–228.
- Rampino M. R., Caldeira K., Zhu Y. A pulse of the Earth: A 27.5-Myr underlying cycle in coordinated geological events over the last 260 Myr. *Geoscience Frontiers*, 2021, v. 12, 101245.
- Catalog of Exoplanets. Observatoire de Paris, <http://exoplanet.eu/>
- NASA Planetary Fact Sheet – Metric (2019).
- Bills B. G., Ray R. D. Lunar Orbital Evolution: A Synthesis of Recent Results. *Geophysical Research Letters*, 1999, v. 26, no. 19, 3045–3048.
- Tiruneh G. Explaining Planetary-Rotation Periods Using an Inductive Method. arXiv:0906.3531, 2009.
- Haisch K. E. et al. Disk frequencies and lifetimes in young clusters. *The Astrophysical Journal*, 2001, v. 553, L153–L156.
- Montmerle T. et al. Solar System Formation and Early Evolution: the First 100 Million Years. *Earth, Moon, and Planets*, 2006, v. 98, 39–95.